

High Vibrational States of Carbon Monoxide in Liquid Argon: Overtone Intensity Enhancement and Reactions with Oxygen

Robert Disselkamp and George E. Ewing*

Department of Chemistry, Indiana University, Bloomington, Indiana 47405 (Received: February 14, 1989)

Isotopic carbon monoxide (88% $^{13}\text{C}^{16}\text{O}$, 12% $^{13}\text{C}^{18}\text{O}$) dissolved in liquid argon was optically pumped to the $\nu = 1$ level by a CW CO laser. This energy spontaneously redistributes by collisional up-pumping to populate high vibrational levels in the $^{13}\text{C}^{18}\text{O}$ isotope. Fluorescence from levels up to $\nu = 37$ in the heavier isotope was observed from the steady-state distribution. First, second, and third overtone fluorescence from high vibrational levels in the $^{13}\text{C}^{18}\text{O}$ isotope were observed. The result of populating high vibrational levels in the $^{13}\text{C}^{18}\text{O}$ isotope has led to the discovery of two phenomena. First, a comparison of the intensity of high overtone fluorescence against calculated gas-phase intensities shows a pronounced fluorescence enhancement due to the liquid environment. Second, CO_2 production was observed from an O_2 -doped CO solution resulting from pumping by the infrared laser. The mechanisms for liquid-state collisional up-pumping, fluorescence enhancement, and infrared photochemical production of CO_2 are discussed.

I. Introduction

Previous studies of up-pumping behavior of CO have been conducted in the gas phase,¹ liquid phase,² and solid phase.³⁻⁶ The gas-phase experiments of Bergman and Rich¹ have shown first overtone fluorescence to occur from vibrational levels up to $\nu = 42$ in the $^1\Sigma_g$ ground electronic state of CO. A vibration to electronic (V-E) energy transfer process populated levels in the $A^1\Pi$ excited electronic state which is isoenergetic with $\nu = 42$ of ground-state CO. This excited electronic state was observed to fluoresce and quench further up-pumping behavior. The formation of CO_2 was observed in this system and is believed to result from reactions between CO molecules. It was not established, however, whether the reaction proceeded through an excited electronic state of CO or high vibrational levels of the $^1\Sigma_g$ ground state. An additional side reaction which formed C_2 was also observed through the $\text{C}_2(A^3\Pi_g \rightarrow X^3\Pi_u)$ Swan band emissions. An overall reaction mechanism and resulting stoichiometry for carbon-13-enriched products in this gas-phase system have been described.⁷ Experiments conducted in this laboratory by Anex and Ewing² have demonstrated up-pumping to the $\nu = 20$ level of CO in liquid argon. Efficient energy transfer occurring from high vibrational levels in CO to trace impurities was shown to terminate further up-pumping. A kinetic model of the steady-state population distribution was used to obtain a value for this quenching rate. Matrix studies conducted by Dubost³ have shown first overtone fluorescence emanating from vibrational levels up to $\nu = 30$. An oxygen impurity in his system allowed V-E energy transfer from high vibrational states in CO to both the $\text{C}^3\Delta_g$ and $\text{b}^1\Sigma_g^+$ molecular states of O_2 . Emission from these O_2 states was observed, and a discussion of the V-E transfer process was given. Legay⁴ has also studied solid-phase systems and has observed a strong population inversion occurring from up-pumping in a solid sample of pure carbon monoxide. The laser excitation source developed by Legay has been used in our studies of energy transfer in cryogenic liquids. An investigation into the theoretical rate of energy flow for optically pumped systems of anharmonic oscillators was initially described by Manz.^{5,6} He described the time evolution of vibrational levels of CO contained in various inert gas matrices. These theoretical models were later used to extract rate constants for various energy transfer processes.

The present study of up-pumping in cryogenic liquids continues to investigate phenomena common in both gas-phase and solid-phase systems, as well as investigating the perturbations caused by solvent molecules on solute species. This paper is organized into the following format. After a brief description of the experimental arrangement, section II, laser pumping of the system is described in section III-1. The conditions for collisional up-pumping of CO dissolved in liquid argon are presented in section

III-2. Section III-3 will examine the measured liquid-phase intensities for the first, second, and third overtones of $^{13}\text{C}^{18}\text{O}$, and a comparison against calculated gas-phase intensities will be given. The fluorescence observed for the liquid system will be shown to be enhanced compared to the same fluorescence calculated for the gas-phase system, and a discussion for this enhancement will be presented. Section III-4 will describe the behavior of an optically pumped liquid argon solution of CO doped with O_2 . The resulting population distribution will be compared with that for up-pumping in a high-purity sample of CO in liquid argon. Finally, section III-5 will describe the photochemistry observed for an O_2 -doped CO solution in liquid argon and propose a mechanism for the production of CO_2 .

II. Experimental Section

A schematic diagram of the experimental apparatus is shown in Figure 1. The laser excitation source was an electrical discharge of flowing $\text{CO-N}_2\text{-He}$ gases, which produces low vibrational transitions in CO when cooled with liquid nitrogen. This output was sent to a beam splitter from which 10% was reflected to a Scientech 36-000 disk calorimeter for continuous monitoring of the laser intensity. The remaining radiation was focused by a 25-cm focal length CaF_2 lens into a cell containing a dilute mixture of CO in liquid argon. The overtone emissions from CO were obtained during continuous excitation of the sample. Fluorescence was collected at a right angle by a spherical mirror used off-axis, modulated at 667 Hz with a mechanical chopper, and focused onto the entrance slit of a Model B210 Perkin-Elmer monochromator equipped with two gratings fastened to a rotating mount. First overtone emission was monitored by using a grating blazed at 3.75 μm , whereas second and third overtone emissions were monitored by using a grating blazed at 1.4 μm . The dispersed fluorescence was focused onto an Infrared Associates InSb photovoltaic detector cooled to 77 K and then sent to a preamp ($\times 1000$). This signal was sent to a Princeton Applied Research (PAR 120) lock-in amplifier and then to a chart recorder for readout.

Frequency calibration of the spectrometer was accomplished by introducing a helium-neon laser source into the monitored fluorescence beam. The helium-neon laser source passing through the monochromator was detected at higher orders on each grating

(1) Bergman, R. C.; Homicz, G. F.; Rich, J. W.; Wolk, G. L. *J. Chem. Phys.* **1983**, *78*, 1281.

(2) Anex, D. S.; Ewing, G. E. *J. Phys. Chem.* **1986**, *90*, 1604.

(3) Galaup, J. P.; Harbec, J. Y.; Charneau, R.; Dubost, H. *Chem. Phys. Lett.* **1985**, *120*, 188.

(4) Legay-Sommaire, N. J.; Legay, F. *IEEE J. Quantum Electron.* **1980**, *QE-16*.

(5) Manz, J. *Chem. Phys.* **1977**, *24*, 51.

(6) Manz, J. *Chem. Phys. Lett.* **1977**, *51*, 477.

(7) Luiti, G.; Dondes, S.; Harteck, P. *J. Chem. Phys.* **1966**, *44*, 4051.

* To whom correspondence should be addressed.

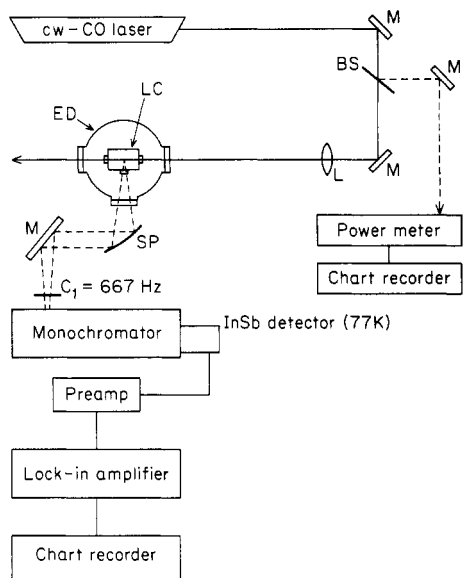


Figure 1. Simplified diagram of the experimental setup for measuring up-pumping in cryogenic solutions: M, mirror; BS, beam splitter; ED, evacuated Dewar; LC, liquid cell; SP, spherical mirror; C_1 , mechanical chopper; L, 25-cm focal length CaF_2 lens.

and used to provide an absolute wavenumber calibration as well as provide spectral resolution information. The resolution was found to have a half-width (fwhh) of 3.0 cm^{-1} , which was adequate for monitoring the diffuse liquid-state fluorescence. The frequency accuracy was determined to be $\pm 3.0 \text{ cm}^{-1}$.

The wavelength-dependent photometric efficiency for the spectrometer was established in order to convert the measured fluorescence features onto a scale that was linear in intensity from 2500 to 6500 cm^{-1} . A globar, whose temperature was not known, was left for 1 h to achieve some steady-state temperature. The temperature was then determined from a Pyro (Model 87) optical pyrometer and shown to be constant. Intensity versus wavenumber scans of the globar source were performed for both the 3.75 - and $1.4\text{-}\mu\text{m}$ gratings. From these scans it was possible to determine the spectrometer relative photometric efficiency by dividing the measured globar intensity by the expected intensity obtained from the Planck blackbody relationship using the globar emissivity versus wavelength properties.⁸ These spectrometer correction factors were tabulated for all transition frequencies of interest and were used together with other wavelength-dependent properties to establish a linear intensity scale for the observed fluorescence features.

The cryogenic brass cell containing the sample, similar to that described previously,² was attached to the bottom of a Dewar and fitted with sapphire windows sealed with indium. Lithium fluoride salt plugs were inserted inside the cell to inhibit absorption of laser light outside the region viewed by the collection optics. The path length of the liquid cell was 0.63 cm . The samples were prepared by filling a known volume to a prespecified pressure of CO. The cell was then cooled by filling the Dewar with liquid argon. Gaseous argon was then condensed into the cell containing CO to form the liquid solution. An accurate determination of the sample concentration was then achieved through FTIR absorption and known integrated absorbance data for CO given by Chandler.¹⁰ Solution concentrations were typically $0.005 \text{ mol } \% \text{ CO}$. Solutions containing O_2 were prepared by first mixing the gas with CO to the appropriate partial pressure.

The Matheson grade argon used (containing $<0.5 \text{ ppm}$ of CO_2 and CH_4 ; $<1.0 \text{ ppm}$ of CO , H_2 , and N_2 ; and 0.2 ppm of O_2) was purified by passing it through a 1-m column of dry ice cooled

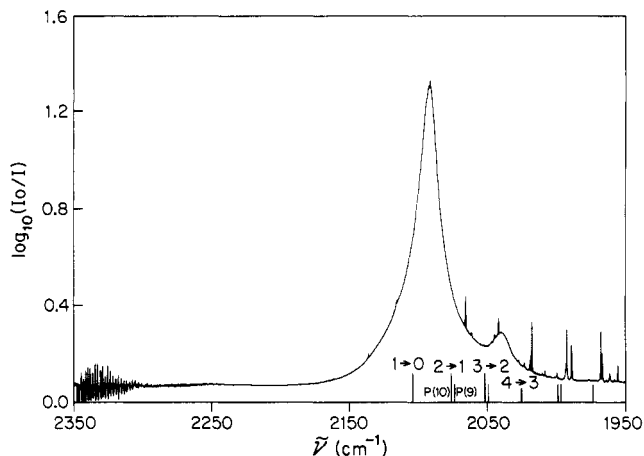


Figure 2. FTIR absorbance of $^{13}\text{C}^{16}\text{O}$ and $^{13}\text{C}^{18}\text{O}$ dissolved in liquid argon. The total $[\text{CO}] = 1.0 \times 10^{19} \text{ molecules cm}^{-3}$. Also shown at the bottom of the figure is a sketch of a typical laser line emission spectra illustrating the overlap with the absorption spectra. Both P(9) and P(10) rovibrational laser transitions are shown.

molecular sieve (Linde type 4A). The isotopically enriched carbon-13 CO from Monsanto contained an isotopic composition (in atom %) of 99.4% carbon-13 and 0.6% carbon-12, with 88% oxygen-16 and 12% oxygen-18. The gross composition in mole percent was 99.12% CO, 0.12% CO_2 , 0.69% Ar, 0.02% H_2 , and 0.05% He. To remove CO_2 , the CO gas was cycled through a mixture of Ascarite (80 wt %) and magnesium perchlorate (20 wt %)¹¹ contained in a test tube sealed to the bottom of a 1-L bulb. Liquid nitrogen cooling of the test tube containing these reagents, followed by heating to approximately $100 \text{ }^\circ\text{C}$, was sufficient for gas purification after five cycles were performed for each sample made.

An investigation into the photochemical CO_2 formation required the preparation of O_2 -doped CO mixtures which were again cycled through Ascarite and magnesium perchlorate to remove any impurity CO_2 present.

The laser source, following the design of Legay,¹² operates on several low vibrational transitions near P(9) and P(10) with a typical output shown within the CO absorption profile given in Figure 2. After maximizing the laser output into the low vibrational transitions, typically 30 mW was observed for the $\nu = 1 \rightarrow \nu = 0$ transition and 150 mW for the $\nu = 2 \rightarrow \nu = 1$ transition. The total output power varied from 1.2 to 2.0 W .

Absorbance spectra were acquired from a Mattson Instruments FTIR (Nova Cygni 120). Comparisons between spectra are shown off-set from one another using the same absorbance scale, and all were obtained with a spectral resolution of 0.125 cm^{-1} .

III. Results and Discussion

1. Laser Pumping the System. Figure 2 shows the absorbance spectra for isotopically enriched CO in liquid argon. The larger absorbance feature located at 2091 cm^{-1} is due to the more abundant $^{13}\text{C}^{16}\text{O}$ isotope, and the smaller absorbance feature at 2039 cm^{-1} is due to the lesser abundant $^{13}\text{C}^{18}\text{O}$ isotope. Atmospheric gas-phase absorptions from water and carbon dioxide are centered around 2000 and 2330 cm^{-1} , respectively. A typical laser line output is also shown at the bottom of Figure 2, illustrating the favorable overlap of the $1 \rightarrow 0$ and $2 \rightarrow 1$ laser emissions within the $^{13}\text{C}^{16}\text{O}$ absorption profile and the less favorable $3 \rightarrow 2$ and $4 \rightarrow 3$ laser emissions located within the $^{13}\text{C}^{18}\text{O}$ absorption profile. During sample excitation this absorbed energy is rapidly exchanged between the two isotopes (eq 1) at a rate comparable to their liquid-phase collision frequency.¹³

(11) Hayes, J. Geology Department, Indiana University, personal communication.

(12) See: Brechignac, Ph.; Martin, J. P. *IEEE J. Quantum Electron.* **1976**, *12*, 80.

(13) Yardley, J. T. *Introduction of Molecular Energy Transfer*; Academic Press: New York, 1980.

(8) *Methods of Experimental Physics*; Williams, D., Ed.; Academic Press: New York, 1962; Vol. 3.

(9) *Building Scientific Apparatus*; Moore, J., Davis, C., Coplan, M., Eds.; Addison-Wesley: Reading, MA, 1983.

(10) Chandler, D. W.; Ewing, G. E. *Chem. Phys.* **1981**, *54*, 241.

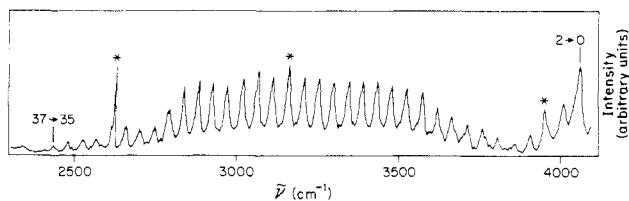
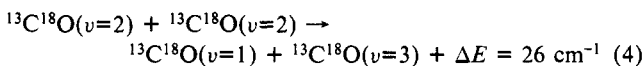
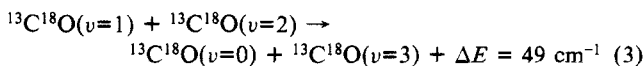
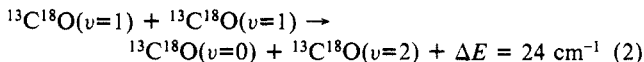
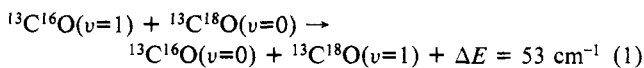


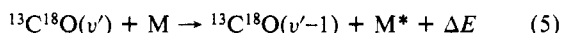
Figure 3. First overtone emission spectra of $^{13}\text{C}^{18}\text{O}$ dissolved in liquid argon. Up-pumping is observed from vibrational levels up to $\nu = 37$. Helium-neon laser calibration lines are indicated by asterisks.

2. Conditions for Collisional Up-Pumping. The phenomenon of up-pumping can be observed in systems that contain anharmonic oscillators when two conditions are satisfied. First, the rates for vibration-vibration (V-V) energy transfer must be faster than all other rate processes, such as vibration-translation/rotation (V-T/R) quenching, radiative losses, and vibration-electronic (V-E) transfer, or relaxation to impurity molecules. A second condition requires that an abundant amount of vibrational energy be supplied to the system for the redistribution process to occur. A discussion of these processes as applied to CO dissolved in liquid argon will now be given.

The dominant energy transfer exchange processes can be written as follows:



⋮



The exothermic nature of these reactions is their driving force, with the excess energy being taken up by the bath. Reaction 1 transfers a fraction of the absorbed laser energy from the $^{13}\text{C}^{16}\text{O}$ isotope to the $^{13}\text{C}^{18}\text{O}$ isotope. With the initial absorbed energy partitioned between the two isotopes,² further exothermic V-V exchange processes occur which populate high vibrational levels in the $^{13}\text{C}^{18}\text{O}$ isotope. This corresponds to reactions 2-4 which redistribute the vibrational energy among many vibrational states in the $^{13}\text{C}^{18}\text{O}$ isotope. Many more exchange reactions not shown contribute to the entire redistribution process. Reaction 5 is a quenching reaction which limits up-pumping to a vibrational level designated here as ν' . Efficient energy transfer occurs between $\text{CO}(\nu')$ and M such that vibrational levels no greater than ν' in CO become populated. Two types of experiments will be discussed in this paper, and each has different quenching processes. For up-pumping in the pure CO solution in liquid argon the quenching process shown in reaction 5 is not important, and the observed up-pumping for this system is limited only by the signal/noise of the detected fluorescence. Bergman and Rich¹ have shown that up-pumping in gas-phase CO occurs up to $\nu = 42$ which then undergoes internal conversion into the $\text{A}^1\Pi$ electronic state followed by fluorescence to low vibrational levels in the ground state, hence effectively terminating any further up-pumping. The same type of interaction between these electronic states may also limit the up-pumping of CO occurring in liquid argon but cannot be confirmed from our data. For up-pumping in the O_2 -doped CO solution in liquid argon, the quenching partner M in reaction 5 is likely to be the O_2 present as we shall discuss in section III-4.

3. Liquid-State Overtone Fluorescence Intensity Enhancement. Figure 3 shows the first overtone emission from the $^{13}\text{C}^{18}\text{O}$ isotope. Fluorescence is observed from every vibrational level starting from the $\nu = 2 \rightarrow \nu = 0$ transition up to and including the $\nu = 37 \rightarrow \nu = 35$ transition. Despite attempts to purge the monochromator

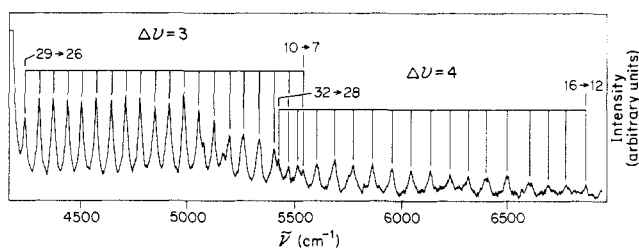


Figure 4. Second and third overtone emission spectra of $^{13}\text{C}^{18}\text{O}$ dissolved in liquid argon. The off-scale $2 \rightarrow 0$ emission feature from the $^{13}\text{C}^{16}\text{O}$ isotope is located at the left-hand side of the figure.

TABLE I: Gas- and Liquid-Phase CO Overtone Intensity Enhancements

ν	gas-phase CO	CO in liquid Ar
	$I_{\nu \rightarrow \nu-2} : I_{\nu \rightarrow \nu-3} : I_{\nu \rightarrow \nu-4}$	$I_{\nu \rightarrow \nu-2} : I_{\nu \rightarrow \nu-3} : I_{\nu \rightarrow \nu-4}$
17	1:0.01:-	1:0.9:0.1
18	1:0.01:-	1:0.9:0.1
19	1:0.01:-	1:0.9:0.1
20	1:0.01:-	1:0.7:0.2
21	1:0.01:-	1:0.8:0.2
22	1:0.01:-	1:0.8:0.2
23	1:0.01:-	1:0.8:0.2
24	1:0.01:-	1:0.8:0.2
25	1:0.01:-	1:1:0.3
26	1:0.01:-	1:1:0.3
27	1:0.01:-	1:1:0.3
28	1:0.01:-	1:1:0.3
29	1:0.01:-	1:1:0.5

and external optics, small atmospheric water absorptions will interfere with the fluorescence as seen from transitions $\nu = 4 \rightarrow \nu = 2$ to $\nu = 12 \rightarrow \nu = 10$. The helium-neon laser calibration features are marked with an asterisk and permit a calibration of the $3.75\text{-}\mu\text{m}$ grating.

Second and third overtone fluorescence from $^{13}\text{C}^{18}\text{O}$ are shown in Figure 4. Second overtone fluorescence was observed from the transitions $\nu = 10 \rightarrow \nu = 7$ to $\nu = 29 \rightarrow \nu = 26$, and third overtone fluorescence can be seen to originate from levels $\nu = 16$ to $\nu = 32$. Two additional weak fluorescence features corresponding to third overtone transitions of $35 \rightarrow 31$ and $36 \rightarrow 32$ are located within the second overtone fluorescence region. The large off-scale fluorescence feature located at the far left side of Figure 4 is due to the $\nu = 2 \rightarrow \nu = 0$ emission from the $^{13}\text{C}^{16}\text{O}$ isotope. The half-widths (fwhh) were found to be constant for each overtone with values of $20 \pm 1 \text{ cm}^{-1}$ for the first overtone, $30 \pm 2 \text{ cm}^{-1}$ for the second overtone, and $40 \pm 4 \text{ cm}^{-1}$ for the third overtone.

Examining Figures 3 and 4, it can be seen that first, second, and third overtone fluorescence were observed for vibrational levels from $\nu = 17$ to $\nu = 29$, inclusive. From each of these vibrational levels it is possible to examine the relative intensities of fluorescence emanating from a particular vibrational level resulting in vibrational quantum changes of $\Delta\nu = -2, -3$, and -4 , respectively (for example, $I_{20 \rightarrow 18} : I_{20 \rightarrow 17} : I_{20 \rightarrow 16}$). Comparing the measured liquid-phase intensity ratios to calculated gas-phase intensity ratios will be an indication of how the liquid environment effects such higher overtone radiative transitions. To accomplish this, the measured spectra must be transformed into absolute intensity ratios by accounting for wavelength-dependent experimental parameters, as described in the Experimental Section. In addition, the differing emission half-widths for the various overtones were also used in constructing the desired intensity ratios of $I_{\nu \rightarrow \nu-2} : I_{\nu \rightarrow \nu-3} : I_{\nu \rightarrow \nu-4}$ for $\nu = 17$ to $\nu = 29$. Table I shows the resulting liquid-phase intensity ratios obtained where the value of $I_{\nu \rightarrow \nu-2}$ has been normalized to unity.

The calculated gas-phase intensity ratios, given in Table I, were obtained from integrated absorbance data¹⁴ and relative spontaneous emission coefficients.¹⁵ This was accomplished through

(14) Vu, H.; Atwood, M.; Vodar, B. *J. Chem. Phys.* **1963**, *38*, 2671.

(15) Lightman, A. J.; Fisher, E. R. *Appl. Phys. Lett.* **1976**, *29*, 593.

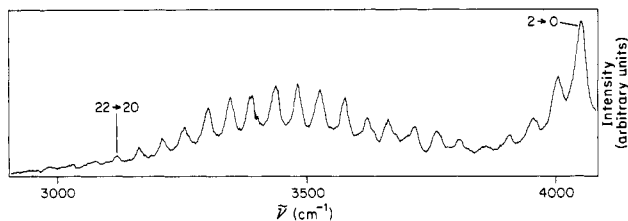


Figure 5. First overtone emission spectra of an oxygen-doped $^{13}\text{C}^{18}\text{O}$ solution dissolved in liquid argon taken during the photochemical formation of CO_2 . The originally doped sample contained 0.5% $^{16}\text{O}_2$ with $[\text{CO}] = 1.1 \times 10^{19}$ molecules cm^{-3} .

the use of the $0 \rightarrow 2$ and $0 \rightarrow 3$ integrated gas-phase absorptions for $^{12}\text{C}^{16}\text{O}$ which were converted to oscillator strengths. These oscillator strengths were then scaled for the $^{13}\text{C}^{18}\text{O}$ isotope, and a radiative rate for the $2 \rightarrow 0$ and $3 \rightarrow 0$ transitions could be obtained.⁸ The next step was to scale these "lowest order" fluorescence rates by their appropriate relative spontaneous emission coefficients and therefore obtain the fluorescence rates for higher vibrational states. Finally, by taking the appropriate ratio of calculated gas-phase fluorescence rates we obtained $I_{\nu \rightarrow \nu-2} : I_{\nu \rightarrow \nu-3}$ for $\nu = 17$ to $\nu = 29$ and by normalizing the first overtone fluorescence rates to unity and rounding to one significant figure the values given for gas-phase CO in Table I were obtained. Since the relative spontaneous emission coefficients have only been calculated for the fundamental, first overtone, and second overtone transitions,¹⁶ it was not possible to calculate the fluorescence rates for the $\Delta v = -4$ gas-phase transitions.

Comparing the first and second overtone intensity ratios in Table I, it can be seen that the liquid-phase intensities are at least an order of magnitude more intense than the corresponding calculated gas-phase intensities. Since we estimate the error to be less than 30% for both systems, the enhancement is much greater than the error involved. Another interesting feature is a trend that exists in the liquid system in that at higher vibrational levels the fluorescence is spread more uniformly over the various overtones.

An explanation for the observed fluorescence enhancement lies in the evaluation of the matrix elements corresponding to these radiative transitions. The preceding intensity ratios can be replaced by

$$\frac{\nu_{\Delta v=2}^3 |\langle \Phi_\nu | \mu(R) | \Phi_{\nu-2} \rangle|^2}{\nu_{\Delta v=3}^3 |\langle \Phi_\nu | \mu(R) | \Phi_{\nu-3} \rangle|^2} : \frac{\nu_{\Delta v=3}^3 |\langle \Phi_\nu | \mu(R) | \Phi_{\nu-3} \rangle|^2}{\nu_{\Delta v=4}^3 |\langle \Phi_\nu | \mu(R) | \Phi_{\nu-4} \rangle|^2} \quad (6)$$

where Φ_ν is the vibrational wave function for state ν and $\mu(R)$ is the electric dipole moment function coupling state ν to state $\nu - 2$, $\nu - 3$, or $\nu - 4$. It can be seen that the enhanced overtone fluorescence in the liquid is due to either a change in the mechanical anharmonicities resulting in different vibrational wave functions or a change in the electrical harmonicity as a consequence of a modification of the electric dipole moment function due to the liquid environment. Since the Franck-Condon factors expected for overtone transitions are quite small, the effective potential for molecules in the liquid will need to be accurately established to give realistic vibrational wave functions. Hence, since it is difficult to model this system, it must suffice to say that either the changed mechanical or electrical anharmonicities result in the observed overtone fluorescence enhancement.

4. Population Distributions. Figure 5 shows the first overtone emission spectra from $^{13}\text{C}^{18}\text{O}$ containing 0.5% $^{16}\text{O}_2$ in CO. By comparing Figures 3 and 5, it can be seen that fluorescence from the undoped sample of Figure 3 was observed from vibrational levels up to $\nu = 37$, whereas fluorescence from the O_2 -doped sample of Figure 5 was observed from vibrational levels only up to $\nu = 22$. The population distributions for $^{13}\text{C}^{18}\text{O}$ in liquid argon for each of these systems can be determined from their respective overtone emission spectra if it is assumed that the first overtone gas-phase spontaneous emission coefficients can be used to describe these liquid systems.

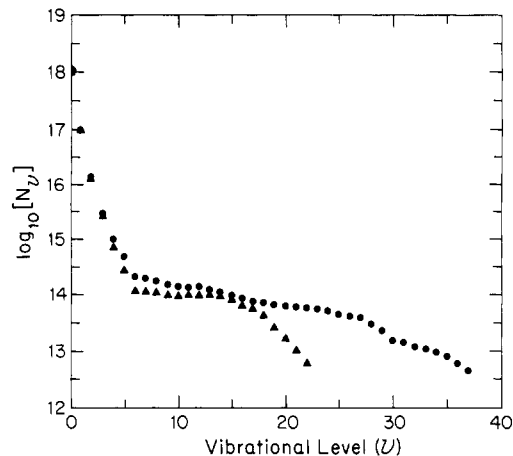


Figure 6. Comparison between the population distributions, given as N_ν in molecules cm^{-3} , obtained for up-pumping occurring in an undoped and O_2 -doped sample of CO dissolved in liquid argon: ●, undoped CO solution; ▲, O_2 -doped solution.

After correcting each integrated emission in Figures 3 and 5 for the wavelength-dependent photometric efficiency of the instrument and then dividing these corrected emissions by their appropriate spontaneous emission coefficients, we obtain the relative concentration of molecules in vibrational levels from $\nu = 2$ to $\nu = \nu_{\text{max}}$. In order to find the concentration of molecules in $\nu = 0$ and $\nu = 1$, it is necessary to introduce a theoretical model proposed by Treanor.¹⁷ The Treanor model describes the redistribution of vibrational energy in systems dominated by V-V exchanges (see eq 1-4) and can be used here to determine the concentration of molecules in $\nu = 0$ and $\nu = 1$. The Treanor function can be written as

$$N_\nu = N_0 \exp(\gamma \nu) \exp[-(E_\nu - E_0)/k_b T] \quad (7)$$

where N_ν is the concentration of molecules in vibrational level ν , E_ν is the $^{13}\text{C}^{18}\text{O}$ vibrational energy, k_b is Boltzmann's constant, T is the system temperature (87 K), and γ is a constant. The parameter γ contained in the first exponential term arises when describing the distribution of vibrational energy among anharmonic oscillators. The value of γ a system achieves can be related to a vibrational temperature² and is a measure of the effectiveness of up-pumping. For the $\nu = 1$ level, this vibrational temperature, θ_1 , is obtained from

$$\gamma = [(E_1 - E_0)/k_b] [T^{-1} - \theta_1^{-1}] \quad (8)$$

The second exponential term in eq 7 is a thermal weighting factor which distributes the vibrational energy. Equation 7 adequately describes the liquid system for low vibrational levels as we have demonstrated in our previous study.² Therefore, from known energy level information, which can be extracted from peak locations in Figure 3, the relative populations of any two low vibrational levels ($\nu = 2$ and $\nu = 3$) can be used to determine γ . With γ determined, it is possible to calculate the relative concentration of molecules in $\nu = 0$ and $\nu = 1$. Weighing the relative populations of all levels by the total number of $^{13}\text{C}^{18}\text{O}$ molecules, it is possible to obtain the absolute steady-state concentrations from $\nu = 0$ to $\nu = \nu_{\text{max}}$ as shown in Figure 6.

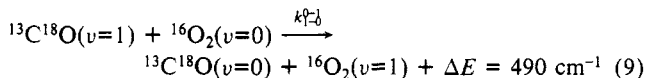
Figure 6 shows a comparison of the population distributions obtained from the first overtone emission spectra of the liquid argon CO solution shown in Figure 3 (illustrated as circles) to that of an O_2 -doped argon CO solution shown in Figure 5 (illustrated as triangles). The undoped sample can be seen to populate vibrational levels up to $\nu = 37$ whereas the O_2 -doped sample populates levels up to about $\nu = 22$, which is consistent with the first overtone spectra of Figures 3 and 5. For populations below $\nu \approx 15$ the distributions for the undoped and O_2 -doped solution are nearly the same. This is reflected in similarities in

(16) Young, L. A.; Eachus, W. J. *J. Chem. Phys.* **1966**, *44*, 4195.

(17) Treanor, C. E.; Rich, J. W.; Rehm, R. G. *J. Chem. Phys.* **1968**, *48*, 1798.

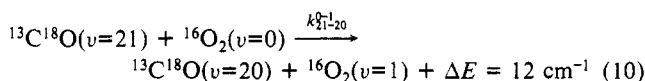
the vibrational temperature being $\theta_1 = 1200$ K for the undoped solution and $\theta_1 = 1250$ K for the O_2 -doped solution.

We can understand the inefficiency of O_2 in changing the system vibrational temperature by comparing the time necessary for vibrational quenching of $^{13}C^{18}O(v=1)$ by O_2 to the lifetime of $^{13}C^{18}O(v=1)$. The lifetime of $CO(v=1)$ in undoped liquid argon is 20 ms^{10} and is a measure of the time allotted to undergo a steady-state vibrational energy redistribution occurring from optical pumping by the infrared laser. If a quenching impurity, e.g. O_2 , is added to the system at such a low concentration that this storage time is not significantly reduced, then the vibrational temperature will not be reduced. The energy mismatch between the low-lying levels of CO and O_2 is fairly large

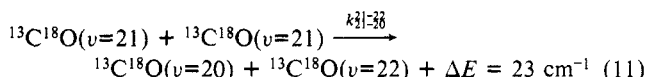


Using the value $k_{1-0}^{0-1} = 1.5 \times 10^{-17} \text{ cm}^3 \text{ molecule}^{-1} \text{ s}^{-1}$ from Williams, Purvis, and Simpson¹⁸ and $[O_2] = 5 \times 10^{16} \text{ molecules cm}^{-3}$ appropriate for our experiment, the storage time is reduced by only 2.7%. We thus have good reason to understand that the low-lying CO levels are efficiently pumped with the addition of a small amount of O_2 .

The situation dramatically changes for the upper vibrational levels as the energy mismatch is closed. For example



is a near-resonant process. This reaction is just a special case of eq 5 we considered earlier. Williams et al.¹⁸ have measured k_{1-0}^{0-1} for reaction 9 for a variety of CO isotopes and find an exponential change in k_{1-0}^{0-1} with energy gap ΔE . A logarithmic extrapolation of this data, consistent with theoretical predictions,¹³ reveals $k_{1-0}^{0-1} \approx 10^{-13} \text{ cm}^3 \text{ molecule}^{-1} \text{ s}^{-1}$. In addition, we introduce a factor of 21 due to the dependence of the rate expression on the matrix element for the $v = 21 \rightarrow v = 20$ quantum change¹⁹ to obtain $k_{21-20}^{0-1} \approx 2 \times 10^{-12} \text{ cm}^3 \text{ molecule}^{-1} \text{ s}^{-1}$. Using k_{21-20}^{0-1} from reaction 10 and V-V exchange rates for CO given by Deleon and Rich,²⁰ it was possible to compare the rate for vibrational quenching of $^{13}C^{18}O(v=21)$ by O_2 to a rate that describes the exchange of vibrational energy among $^{13}C^{18}O(v=21)$. The dominant exchange reaction, a special case of eq 3 or 4, is



has a value $k_{21-22}^{0-1} \approx 1 \times 10^{-9} \text{ cm}^3 \text{ molecule}^{-1} \text{ s}^{-1}$.²⁰ Using $[^{13}C^{18}O(v=21)] \approx 8 \times 10^{13} \text{ molecules cm}^{-3}$, we find the rate of depletion of $^{13}C^{18}O(v=21)$ by O_2 quenching to be comparable (within a factor of 2) to its rate of depletion to produce higher vibrational levels. The abrupt drop in N_v at high vibration levels of CO in the O_2 -doped system can therefore be rationalized from a one-quantum V-V transfer processes.

5. Photochemistry. From studying up-pumping in multicomponent systems, it is possible to examine energy transfer processes not possible in systems that either are at thermal equilibrium or possess single-photon excitation. The main reason for this is that since the system energy, which is contained in one or more of the components present, is distributed over a range of vibrational quantum states, it is possible to satisfy both the resonance condition necessary for rapid energy exchange processes and the activation energy requirements for kinetic processes. In this investigation, the O_2 -doped CO system both has demonstrated an energy exchange process between CO and O_2 and has also undergone reactions that have formed CO_2 . The spectroscopy which involves the CO_2 product will be discussed followed by a proposed reaction

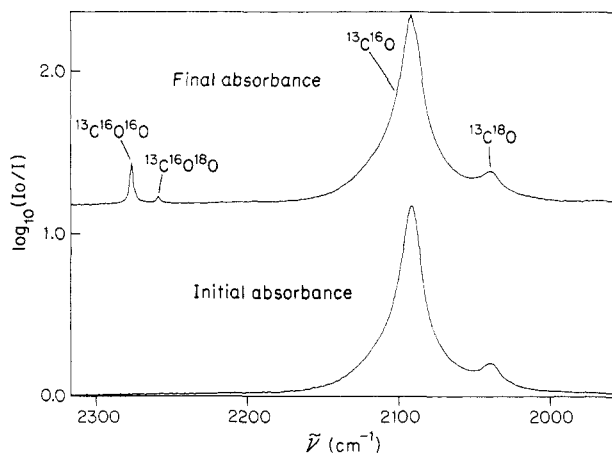


Figure 7. An FTIR absorption of the O_2 -doped CO solution in liquid argon before and after laser irradiation for approximately 1 h shows the formation of isotopic CO_2 species. The concentration of CO_2 species formed is $4.3 \times 10^{16} \text{ molecules cm}^{-3}$.

mechanism to explain its formation.

Figure 7 shows the initial and final absorbance data for an O_2 -doped CO sample. Before laser excitation the only absorbing species are $^{13}C^{16}O$ and $^{13}C^{18}O$. After laser excitation for 1 h, CO_2 formation is apparent. The absorbances of the asymmetric stretch frequencies for CO_2 in liquid argon in Figure 7 occur at 2276.2 cm^{-1} for the $^{13}C^{16}O^{16}O$ isotope and 2257.7 cm^{-1} for the $^{13}C^{16}O^{18}O$ isotope. Both transitions are red-shifted from their respective gas-phase values²¹ by 6.5 cm^{-1} .

The total CO_2 concentration shown in Figure 7 can be determined if it is assumed that the oscillator strength for CO_2 contained in liquid argon is the same as its oscillator strength in the gas phase. Other work with CO_2 in the condensed phase suggests an error of less than 30% in applying this assumption.²² Using the integrated cross section $\bar{\sigma} = 1.1 \times 10^{-16} \text{ cm molecule}^{-1}$,²³ and the Beer-Lambert law with the cell path length equal to 0.63 cm, we arrive at a number density for CO_2 of $[CO_2] = 4.3 \times 10^{16} \text{ molecules cm}^{-3}$ for the data in Figure 7. With $[Ar] = 2.1 \times 10^{22} \text{ molecules cm}^{-3}$, the density of liquid argon, this corresponds to a CO_2 concentration of 2.0 ppm. To determine whether this is the solubility limit of CO_2 in liquid argon at 1 atm, other experiments had to be conducted. In these experiments varying amounts of CO_2 were condensed in liquid argon, and from FTIR absorbance spectra taken at timed intervals it was possible to track the CO_2 concentration as a function time. Samples that were prepared with CO_2 concentrations less than 2.0 ppm showed no change in concentration with time whereas samples prepared with a concentration greater than 2.0 ppm showed a monotonic decrease in the CO_2 concentration until a value of 2.0 ppm was reached. This value is consistent with extrapolations of CO_2 solubilities in liquid argon at higher temperatures.²⁴ Therefore, the CO_2 concentration in Figure 7 is at its solubility limit.

In other experiments we have studied the rate of CO_2 formation with time and have shown that the rate of CO_2 production is roughly constant up to its solubility limit. By extracting the slope of CO_2 formation versus time for these experiments, combined with values for the average laser intensity and the fraction of photons absorbed by the system, it was possible to estimate the quantum efficiency for CO_2 production. The result of such a calculation has shown that it takes approximately 10^3 absorbed photons to produce one CO_2 molecule. The production of CO_2 is an inefficient process.

By relating the composition of the CO_2 products to the composition of the CO present prior to any reactions, it is possible

(18) Williams, H. T.; Purvis, M. H.; Simpson, C. J. S. M. *Chem. Phys.* **1987**, *115*, 7.

(19) *Molecular Vibrations: The Theory of Infrared and Raman Vibrational Spectra*; Bright, W. E., Decius, J. C., Cross, P. C., Eds.; McGraw-Hill: New York, 1955.

(20) Deleon, R. L.; Rich, J. W. *Chem. Phys.* **1986**, *107*, 283.

(21) Herzberg, G. *Infrared and Raman Spectra of Polyatomic Molecules*; Van Nostrand Reinhold: New York, 1945.

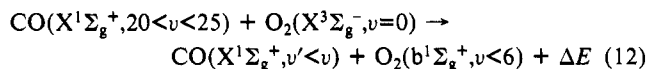
(22) Yamada, H.; Person, W. B. *J. Chem. Phys.* **1964**, *41*, 2478.

(23) *Quantitative Molecular Spectroscopy and Gas Emissivities*; Addison-Wesley: Reading, MA, 1959.

(24) Preston, G.; Funk, E.; Prausnitz, J. J. *Chem. Phys.* **1971**, *75*, 2345.

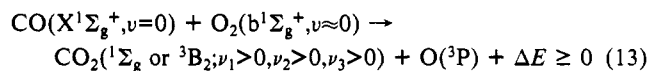
to determine whether any isotope enrichment has taken place. The initially doped sample contained natural abundance O₂ (99.8% ¹⁶O). The CO assay was 88% ¹³C¹⁶O and 12% ¹³C¹⁸O. The observed ratio of ¹³C¹⁶O:¹³C¹⁶O:¹³C¹⁸O is the same as the CO ratio of ¹³C¹⁶O:¹³C¹⁸O. Therefore, a non-isotope-selective method for CO₂ formation must be present since no isotope enrichment is observed. This result will be used when proposing a reaction mechanism for the CO₂ formation.

The effect that O₂ has on up-pumping in ¹³C¹⁸O in liquid argon was discussed in detail in section III-4. Dubost³ has proposed the following reaction to explain visible fluorescence occurring from O₂ contained as an impurity in his matrix-isolated CO system:



This reaction implies that a one-step multiquantum V-E exchange process is populating vibrational levels of the b¹Σ_g⁺ excited electronic state of O₂ with the corresponding decrease in vibrational quanta from CO. Dubost points out only that the net result of populating the b¹Σ_g⁺ state in O₂ occurs. The actual process may be the one-step V-E process just described or many one-quantum V-V exchanges to produce O₂(X³Σ_g⁻, v ≈ 20) followed by internal conversion in O₂. In section III-4 we suggested that one-quantum V-V exchanges from CO to O₂ occur and can explain the decreased concentration of CO near v = 20. These calculated one-quantum exchanges to O₂, however, are not sufficient evidence that O₂(b¹Σ_g⁺) is becoming populated through the internal conversion process. In any event O₂(b¹Σ_g⁺) production is important because it provides a mechanism for the CO₂ formation in the liquid system. Another important consideration is the fluorescence lifetime of O₂(b¹Σ_g⁺) present as solid O₂ has been estimated to be ≈ 1 s;²⁵ therefore, chemistry resulting from this long-lived state is possible.

Investigations into the combustion kinetics of CO by O₂ conducted by Sulzmann and others^{26,27} have determined that the activation energy between CO and O₂ to produce CO₂ is 16 700 cm⁻¹. Since the energy of O₂(b¹Σ_g⁺, v=0) is 36 900 cm⁻¹, an allowed second step in the CO₂-forming reaction sequence is



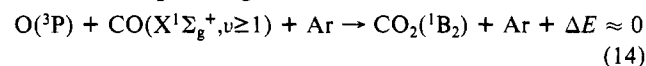
(25) Akimoto, H.; Pitts, J. N. *J. Chem. Phys.* **1970**, *53*, 1312.

(26) Sulzmann, K. G. P.; Meyers, B. F.; Bartle, E. R. *J. Chem. Phys.* **1965**, *42*, 3969.

(27) Brokaw, R. S. *Symp. (Int.) Combust., [Proc.], 14th 1967*, 1063.

The energy of the reaction products in reaction 13 will contain contributions from both the initial internal energy of O₂ and the enthalpy of reaction (ΔE = -2970 cm⁻¹) to yield reaction products with some 39 900 cm⁻¹ of energy. Clyne and Thrush²⁸ have proposed a potential energy diagram for CO₂ which can be used to explain how CO₂ will absorb various reaction enthalpies. These potential surfaces indicate that the 39 900 cm⁻¹ of reaction energy enthalpy generated from reaction 13 will leave the CO₂ product species either in highly excited vibrational levels of its ground electronic state or in its ³B₂ first excited electronic state. This energy is expected to be dissipated by either fluorescence to the ground state or relaxation of the low-frequency bending modes in an efficient manner.

Slinger, Wood, and Black²⁹ have studied the reaction of O(³P) atoms with CO in the presence of an argon buffer gas and have calculated an activation energy of 1520 cm⁻¹ for the process. Requiring that CO possess at least one quantum of vibrational energy will satisfy this activation energy requirement so that an additional CO₂ forming reaction can be written



Reaction 14 produces CO₂ with 44 350 cm⁻¹ of reaction enthalpy which implies that CO₂ will be in its second excited electronic state. It is again expected that CO₂ will dissipate this energy through one of many possible channels.

In summary, reactions 12-14 seem plausible in explaining the CO₂ products observed for three reasons. Reaction 12, which initiates the reaction sequence, has been observed previously in a similar system.³ From this reaction it is necessary only to take the energy contained in O₂ and through a stepwise process from the desired CO₂. Another continuity in the above mechanism is that the majority of the activation energy for these reactions is supplied from reaction 12. In other words, it is not necessary for any additional energy to be supplied to the system in order to drive these reactions once the excited state of O₂ has been populated. Finally, the requirement that the CO₂ products not be isotopically enriched automatically follows from the initiation step given in reaction 12.

Acknowledgment. This work was funded through a grant from the National Science Foundation.

Registry No. CO, 630-08-0; C¹³, 14762-74-4; O¹⁸, 14797-71-8; O₂, 7782-44-7; CO₂, 124-38-9; Ar, 7440-37-1.

(28) Clyne, M. A. A.; Thrush, B. A. *Proc. R. Soc. London, A* **1962**, *269*, 404.

(29) Slinger, T. G.; Wood, B. J.; Black, G. J. *J. Chem. Phys.* **1972**, *57*, 233.